SSRG International Journal of Mechanical Engineering
ISSN: 2348-8360/ https://doi.org/10.14445/23488360/IJME-V13I2P103

Volume 13 Issue 2, 22-32, February 2026

Original Article

Optimizing Deposition Parameters in Friction Surfacing of Al–Ni on Mild Steel

Vinodh Sivalingam[1], Pradeep R[2], Gowtham S[3], Mallireddy Naresh[4]

[1]*Department of Mechanical Engineering, Rathinam Technical Campus, Coimbatore, Tamil Nadu, India.*
[2]*Department of Agricultural Engineering, Sethu Institute of Technology, Viruthunagar, Tamil Nadu, India*
[3]*Department of Mechanical Engineering, Sri Eshwar College of Engineering, Coimbatore, Tamil Nadu, India.*
[4]*Department of Mechanical Engineering, Aditya University, Andhra Pradesh, Tamil Nadu, India.*

[1]*Corresponding Author : vino.infomech@gmail.com*

Received: 18 November 2025 Revised: 20 December 2025 Accepted: 19 January 2026 Published: 20 February 2026

Abstract - *This study focused on the Friction Surfacing (FS) of Al7075–15Ni composite on Mild Steel Substrate (AISI 1018), and the subsequent process parameter were optimized through Taguchi's L9 orthogonal array design. Several distinct permutations of the parameters were investigated to determine their effect on coating quality, to determine the conditions that provide a uniform deposit free from defects, and to determine how the coating dimensions would be altered with changing processing parameters. The thermal behavior during FS was monitored through an instantaneous infrared thermometer by recording the interface temperature at 10-second time intervals. The EDS analysis on the coating deposit confirmed the presence of Fe-Al and Al-Ni intermetallics at the point where the FS layer meets the substrate. The intermixed substrate and coating elements at the contact zone provided a clear indication of diffusion in active mode, showing a strong metallurgical bond across the interface.*

Keywords - *Friction Surfacing, Al-Ni composite, Taguchi's optimisation, Grain refinement, Diffusion.*

1. Introduction

The surface modification process has now become one of the indispensable methods for prolonging the service life and performance of engineering materials, which are intended primarily to become significant wear, corrosion, and thermal loading barriers while maintaining the intrinsic properties of the base material in the process [1]. Conventional coating techniques such as TIG cladding, plasma spray, and thermal spray are commonly utilised for Al–Ni deposition on steel; however, this fusion and powder-based coating process may frequently introduce various defects, such as porosity, oxide entrapment, interfacial cracks, and residual stresses due to thermal mismatch and melting–solidification cycles [2, 3]. Being one of the methods, Friction Surfacing (FS) has caught considerable interest as a solid-state coating method, able to produce dense, defect-free layers and strong metallurgical bonding [4, 5]. The consumable revolves and moves towards the substrate under a provided axial load in this process. Friction heating softens the rods' material before being transfer-filmed as a covering over the substrate [6, 7]. FS is superior to conventional fusion-based coating techniques in terms of minimal dilution, porosity, and cracking, in addition to integrity and adhesion. Generally, FS offers good coating integrity, bonding strength, and refined grain structure [8]. Aluminium-based metal matrix composites used for coating usually improve the mechanical, thermal, and chemical properties of low-carbon steel [9-11]. Aluminum-Nickel Alloys have become much-admired coating materials for their tremendous resistance to oxidation, really good durability, and low density, coupled with the ability to form stable intermetallic phases like Al_3Ni [12, 13]. These intermetallics are known to enhance hardness and thermal stability; thus, making the Al-Ni coatings much suited for extreme conditions in structural, automotive, and aerospace applications [14, 15]. Prior investigation in Al-Ni coating shows an improvement in surface hardness through Al_3Ni/Al_3Ni_2 intermetallic formation, but also highlights an adhesion loss and microstructural inhomogeneity, leading to solidification shrinkage and brittle phase [16]. Mild steel, though commonly used in industrial and structural sectors, is usually limited by poor wear and corrosion resistance [17]. The deposition of an Al-15Ni alloy onto mild steel using FS is a viable facility for overcoming such limitations and improving surface functionality to prolong its service life. Process parameters are key determinants of the quality and performance of FS coatings. Incorrect parameter selection leads to coatings that are non-uniform, weakly adherent, or exhibit dimensional defects [18]. Systematic optimization procedures have to be applied to remedy these conditions. The Taguchi method, based on an L9-orthogonal array, has been widely used for the

optimization of FS parameters. FS of AA2014 on low-carbon steel with different consumables (AA2014, SS316, D3 tool steel) showed that rotational and traverse speeds are very influential in coating geometry and adhesion [19].

The forging pressure plays the key role in shaping the coating from beginning to end in the process. Experimental results showed that both coating width and depth decrease with increasing spindle speeds and feed rates. However, if such parameters exceed certain limits, proper deposition does not occur because the consumable rod would slide over the substrate without sufficient heat generation [20, 21]. Among other things, interfacial diffusion helps to create a composite-like structure that enhances both mechanical integrity and thermal reliability of the covering [22, 23].

The thermal phenomenon is an essential characteristic of FS, essential in determining interface temperature for plastic flow, diffusion of material, and bonding quality. It is also important for determining the shape and mechanical properties of coatings produced through FS. Real-time infrared thermometry will provide a non-contact method for monitoring interface temperatures between tool and workpiece, which consequently correlates thermal input to coating behavior [24]. Too much heat causes thick and brittle intermetallics, while too little leads to weak adhesion or incomplete deposition. Temperature at the interface is generally reported to range between 500°C and 900 °C with variations due to tool speed, traverse rate, and axial load [25, 26]. The process variables highly influence the geometry of the coating deposit. While too much load may reduce coating thickness due to material squeeze out, high axial load is often observed to promote coating width from increased lateral flow of plasticized material [27, 28]. The plasticization is, however, revolution speed dependent; too high speeds mostly yield thinner deposits and flash losses, while moderate speeds create homogeneous deposits. An increase in traverse speed reduces the deposition time per unit length, thus leading to thinner, but sometimes narrower, coatings [29, 30].

Many coating techniques (Thermal Spray, Plasma Spray, Hot Dip, Cladding, etc) involve melting or high-temperature solidification, often causing porosity, surface cracks, oxide formation, residual stresses, and weak metallurgical bonding. Prior studies on Al–Ni coatings deposited by fusion-based or powder-based routes report intermetallic formation but also highlight defects such as interfacial cracks and limited adhesion due to thermal mismatch and solidification shrinkage. A small overview of literature findings, along with limitations and research gaps, is presented in Table 1.

Table 1. Brief literature review: major findings, limitations, and research gap

Coating Technique	Key Findings	Limitations Identified	Research Gap Identified
Fusion-based thermal spraying of Al-Ni coatings [2, 3].	Achieved Al-Ni coating with improved wear resistance.	High porosity and solidification cracking due to melting and rapid cooling were observed.	The fusion-based coating failed to produce dense, non-cracked Al-Ni coatings with strong metallurgical bonding.
Al–Al-Ni coating on steel substrates by laser cladding [13, 31].	Increased hardness through intermetallic formation.	Dilution and residual stresses caused by excess heat input	Controls on heat-cycle effects and interfacial diffusion are lacking.
Cold spray Al composite-based coatings [32].	Reduced oxidation and porosity compared to thermal spray.	Weak interfacial bonding strength with steel substrates.	Inadequate metallurgical bonding due to insufficient thermal activation.
FS of aluminium alloys [33].	Demonstrated solid-state deposition with refined microstructure.	Focus limited to single-material systems without compositional complexity	Absence of studies on composite or intermetallic Al–Ni systems using FS.
FS parameter studies [24]	Identified the influence of vertical forging force and tool rotation speed on coating quality.	Thermal behaviour and dimensional effects were not analyzed.	No integration of parameter optimization with thermal analysis.
Al–Al-Ni intermetallic coatings by fusion-based route [34].	Improved high-temperature performance.	Weak adhesion and micro-crack formation at the interface.	Need for a solid-state route to avoid fusion-related defects.

Very few works investigate Al–Ni composite coating, and no studies report on solid state FS deposition with optimized parameter selection through coupled thermal modelling, parameter effect on dimensional quality, phase validation, and microstructural integrity. Also, the behaviour of Fe–Al intermetallics or Al–Ni intermetallics and the process of substrate–coating intermixing under the various FS parameter combinations are often not well understood, especially when using the parameter optimization framework. This study bridges the gap through the integrated investigation of FSed Al–Ni composite coatings on low carbon steel, where process parameters are optimised, and parameter impact on coating dimension is assessed. Unlike other existing coating research on FS, this work uniquely correlates coating thickness, substrate dimension influence, heat-cycle behaviour, and interfacial diffusion with crystallographic phase confirmation and characterization with EDS line mapping. The results demonstrate that optimized FS parameters produce dense coatings with strong metallurgical bonding, overcoming limitations reported in fusion-based Al–Ni coatings such as porosity, cracking, and weak adhesion.

2. Materials and Methodology

AISI 1018 mild steel plates measuring 100 × 50 × 20 mm served as the substrate. The consumable rod Al7075-15 wt.% Ni composite was prepared from a stir casting process; fabricated casting is machined into cylindrical rods of diameter measuring 20 mm and 150 mm length. Prior to FS, all substrates were mechanically polished using emery sheets, cleaned with acetone, and dried to remove surface contaminants.

Fig. 1 During FS of Al7075-15 Ni over mild steel substrate

A customized vertical milling machine with a revolving consumable rod holder and an adjustable clamping fixture for substrate security was used to perform FS studies. The primary process parameters considered in this research include the applied Axial Pressure (bar), The Substrate Travel Speed – Linear Motion(mm/min), and The Coating Rods' Rotational Speed (rpm). Before additional characterization, coating thickness, width, and bonding quality were visually examined, and each experiment was conducted twice to guarantee reproducibility. Once sufficient heat from friction had been generated, the substrate was driven linearly to deposit the Al–15Ni layer. Figure 1 depicts the FS of Al7075-15Ni across the base material. To optimize this process, Taguchi's L9 orthogonal array was used. Axial Force (Vertically Downward), Traverse Speed (Horizontal Direction), and Coating Rod Rotational Speed were the three key variables that were selected, each having three different levels. In order to examine the impact of process factors, geometric dimensions and coating quality were employed as response variables.

Wire EDM was used to section the deposited coatings perpendicular to the surface. Standard metallographic techniques were used to mount, grind, and polish cross-sectional samples before they were etched in Keller's reagent. The elements distribution and interface composition between the material to be coated and the FS deposit were investigated using EDS that was connected to the SEM. The sample that was prepared for EDS analysis is presented in Figure 2. Using image analysis software, coating geometry, such as thickness and width, was measured from the cross-sectional micrographs.

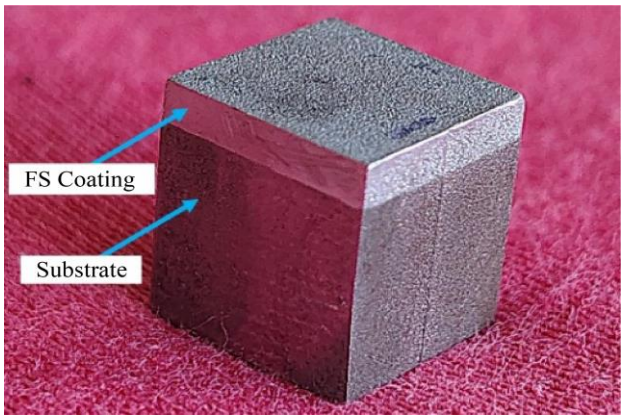

Fig. 2 Sample prepared for EDS analysis

During FS, a non-contact infrared thermometer (accuracy ±1 °C, range up to 1200 °C) was used to measure the interface temperature. To get a precise surface temperature without making physical contact, the thermometer was positioned perpendicular to the tool–substrate interface. Throughout the deposition process, measurements were taken every ten seconds. In order to comprehend the thermal influence on coating creation, the temperature evolution profiles were then connected with coating size and quality.

3. Results and Discussion

3.1. Optimization of FS Coatings: A Parametric Investigation

In AA7075-15Ni FS, a Taguchi L9 design was employed with three factors—axial pressure (4.5, 5, 6 bar), spindle speed (1400, 1500, 1550 rpm), and feed rate (35, 50, 55 mm/min)—each tested at three levels. The observations from each experimental condition, along with acceptance status based on visual inspection and coating integrity, are summarized in Table 2. Figure 3 shows the FS performance for various parameter combos. During FS, applied pressure is essential for regulating the consumable material's plastic flow. The coatings were either confined to a small region, had uneven deposition, or displayed discontinuities with ripple patterns and bead forms at a lower pressure of 4.5 bar (S-1 to S-3). These shortcomings point to inadequate material diffusion and plastic deformation, which result in undesirable deposits [35]. Coating uniformity was much enhanced by raising the pressure to 5 bar (S-4 to S-6). S-4 and S-5 were able to provide continuous and uniform deposition with appropriate overlay over the bead. The coating quality was not improved by increasing the pressure further to 6 bar (S-7 to S-9); instead, deposits became thin, flat, discontinuous, or insufficiently coated, most likely as a result of excessive material squeeze-out and inadequate bonding time.

The spindle speed has a direct impact on the consumable rod's plasticization and heat production. As seen in S-4 and S-5, moderate speeds (1500 rpm) promoted uniform and continuous coatings, but lower speeds (1400 rpm) frequently produced limited or thin deposits. Coatings tended to become uneven, non-uniform, or discontinuous at higher speeds (1550 rpm) (S-3, S-6, S-9), indicating that too much rotating energy may cause material loss through flash generation and decreased deposition thickness.

The pace at which material is delivered to the substrate is determined by the consumable feed rate. Assuring continuous deposition requires a balanced feed rate. High feed rates (55 mm/min) in S-3, S-7, and S-9 resulted in non-uniform or discontinuous coatings, while low feed rates (35 mm/min) in S-1, S-6, and S-8 produced thin overlay or restricted coverage. The optimum coating quality was achieved with 5 bar pressure, followed by moderate spindle speed (1400 and 1500), and an ideal feed rate of 50 and 55 mm/min (S-4 and S-5).

Fig. 3 Process parameters influence on the appearance of AA7075-15Ni FS coating

Table 2. Performance outcomes of the FS deposit under the varying process parameters

Exp No.	Axial Pressure (bar)	Rotation Speed (rpm)	Feed rate (mm/min)	Observation	Acceptance Status
S-1	4.5	1400	35	The coating was confined to a limited area.	No
S-2	4.5	1500	50	The coating was uninterrupted but varied in thickness.	No
S-3	4.5	1550	55	A non-uniform deposit showing discontinuity with ripple patterns and bead formations.	No
S-4	5	1400	50	The layer exhibited continuous and uniform thickness.	Yes
S-5	5	1500	55	The deposit showed continuous and even thickness with proper overlay across the bead.	Yes
S-6	5	1550	35	An uneven layer with an insufficient, thin overlay.	No
S-7	6	1400	55	A thin, flat layer with an extended spread across the substrate.	No
S-8	6	1500	35	The coating exhibited inadequate coverage and poor quality.	No
S-9	6	1550	50	Discontinuous layer with irregular formation.	No

3.2. FS Parameter Combinations' Impact on Coating Dimensions

The dimensional characteristics of the FSed AA7075-15Ni coatings, namely width and thickness, have been measured for nine different combinations of axial pressure applied, consumable rotation speed, and feed rate. The results can be summarized in Table 3. The data depicted prominent trends with regard to the relation of the process parameters to the geometry resulting from the coatings.

The application of pressure heavily influences the flow and deposition of the consumable material. At lower pressure (4.5 bar), sample S-1 did not yield a measurable coating, indicating insufficient plasticization and poor surface spread of the material.

With a moderate increase in pressure to 5 bar (S-4 to S-6), coating formation has been regular at widths of between 19.98 mm and 20.82 mm and thickness in the range of 2.18 mm and 2.32 mm.

A further increase to 6 bar (S-7 to S-9) produced wider coatings in some cases (up to 21.05 mm for S-7). However, thickness generally decreased, suggesting that excessive pressure causes material to spread more laterally than vertically, resulting in thinner layers.

Spindle speed governs heat generation and plastic flow of the consumable rod. Moderate speeds (1500 rpm, S-2, S-5, S-8) produced relatively uniform widths (~19.64–19.98 mm) and thickness (~2.14–2.43 mm), indicating a balanced plasticization.

Higher spindle speeds (1550 rpm, S-3, S-6, S-9) led to slightly increased widths (up to 20.82 mm) but reduced thickness (down to 2.04 mm), likely due to increased flash formation and excessive lateral spread of the softened material.

Table 3. Parameter effect on coating dimensions

S. No	Samples	Width(mm)	Thickness(mm)
1	S-1	NA	NA
2	S-2	19.82	2.43
3	S-3	20.10	2.44
4	S-4	20.06	2.30
5	S-5	19.98	2.32
6	S-6	20.82	2.31
7	S-7	21.05	2.15
8	S-8	19.64	2.14
9	S-9	19.76	2.04

The consumable feed rate determines the material supply per unit length of travel. Lower feed rates (35 mm/min, S-1, S-6, S-8) produced either no measurable deposit (S-1) or thick coatings (2.31mm). Higher feed rates (55 mm/min, S-3, S-5, S-7) generally increased coating width slightly (up to 21.05 mm) but did not constantly improve thickness, as high feed combined with high spindle speed or pressure can lead to lateral material spread rather than vertical build-up [36-38]. The study demonstrates that coating width increases with higher pressure and spindle speed, while thickness is maximized at moderate pressure and speed with balanced feed rates. For the optimal dimensionality of the coatings, parameters must be selected carefully to balance lateral flow and vertical deposition. The provided findings enable the

realization of uniform, defect-free FS coatings with the desired geometrical characteristics.

3.3. EDS Analysis on Al-Ni Coating

In the developed EDS profile of AA7075-15Ni deposit, intermetallics such as Al-Ni and Fe-Al are seen at the contact region in Figure 4 (a), promoting bonding by means of metallurgical reaction. In Figure 4 (b), it further describes the intermixing of substrate and coating constituents, where the diffusion of Al and Ni into Fe provides a good anchorage at the interfacial level and enhances the bond integrity. This diffusion-assisted mechanism contributes significantly to the mechanical integrity and adhesion of the coating [39-41]. The amount of Ni reinforcement within the deposited layer is noticed in Figure 4 (c). The fairly evenly dispersed Ni contributes to enhancing the coating's toughness and resistance towards corrosion, although minor aggregates are formed without any remarkable loss in homogeneity. Intermetallic compound formation, elemental interdiffusion, and uniform reinforcement distribution imply the effectiveness of FS for producing thick and adherent coatings.

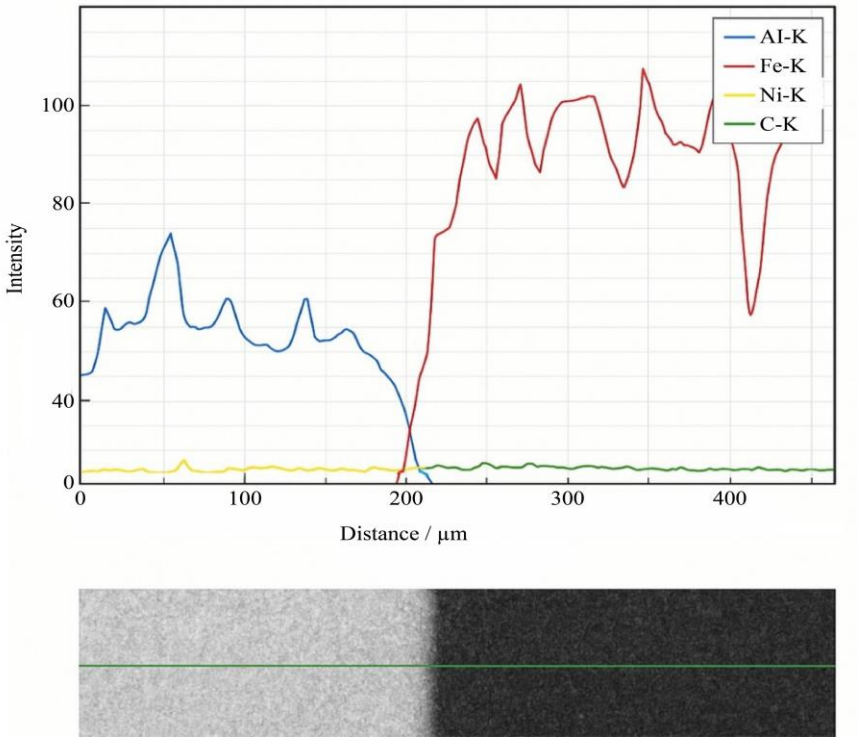

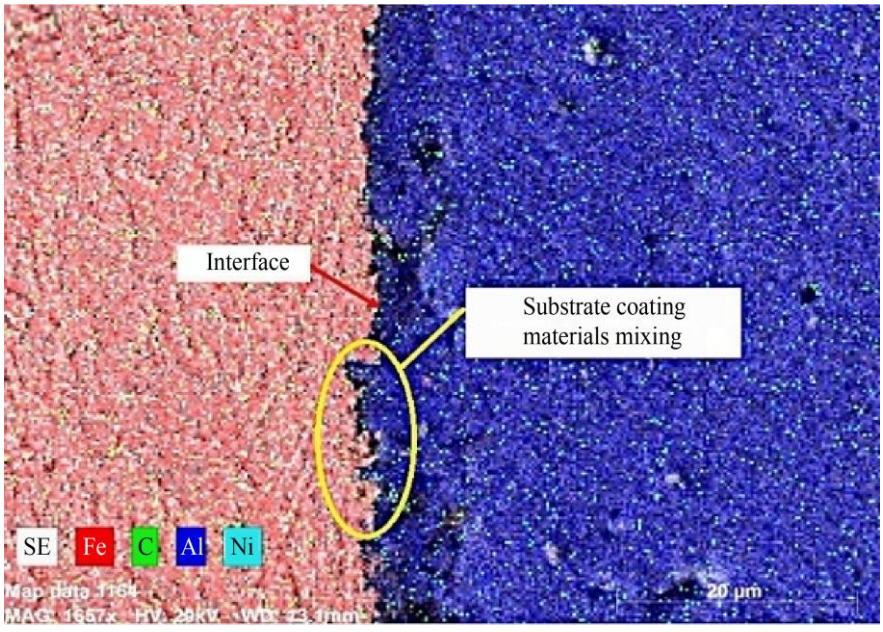

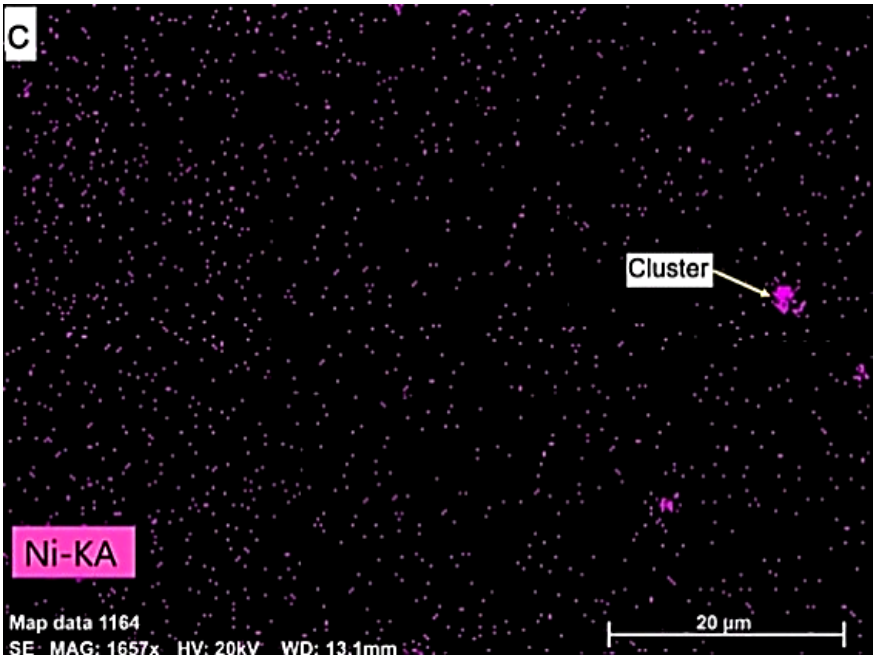

Fig. 4 EDS examination: (a) Line scan across the substrate and coating, (b) Mapping of substrate and the coating material at the interface region, and (c) Distribution of nickel over the coating surface.

3.4. XRD Analysis

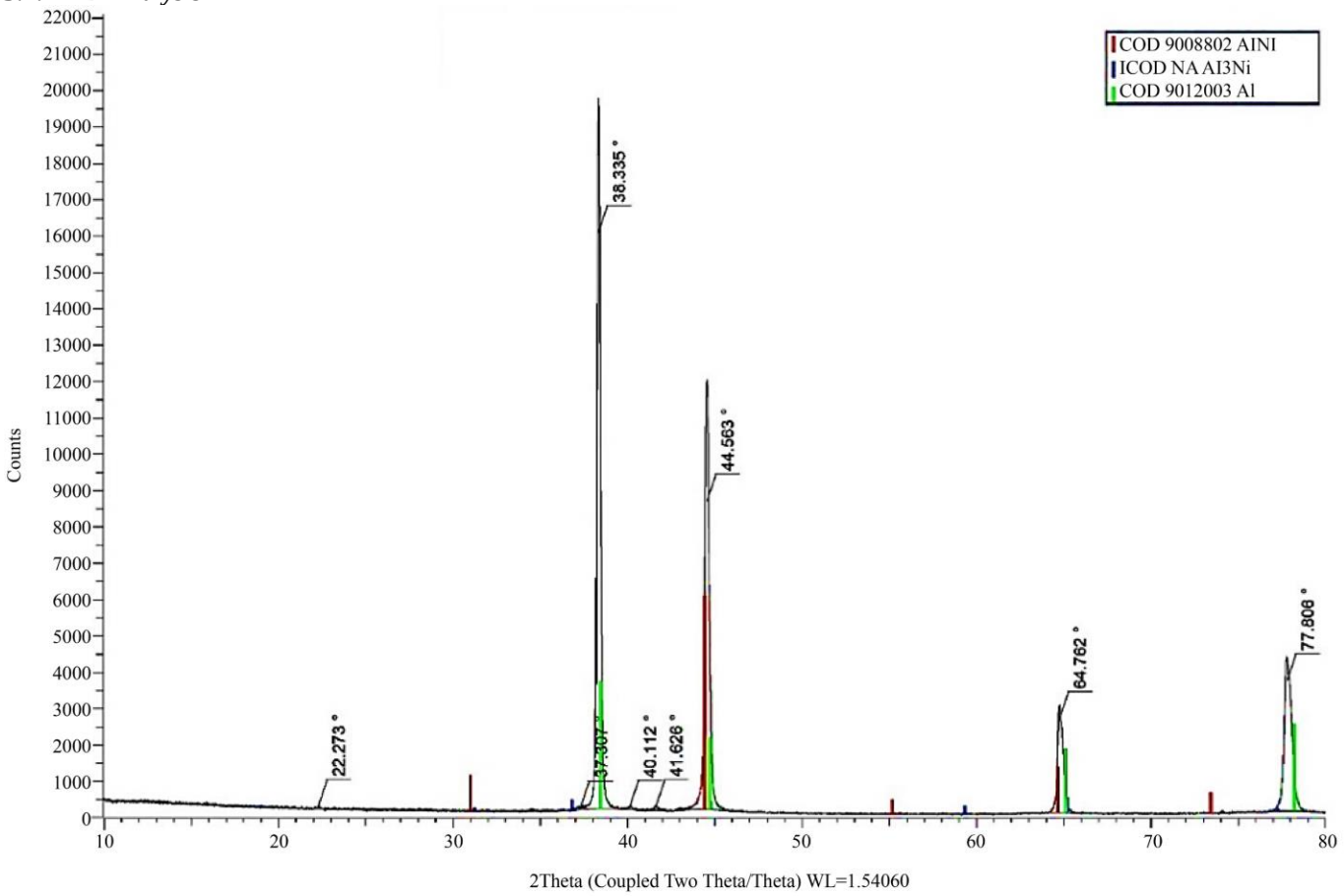

Fig. 5 XRD analysis on FS coating of Al-Ni

The XRD analysis of the FS coating is shown in Figure 5, confirming the presence of Al, AlNi, and Al_3Ni as the three phases based on their respective COD reference patterns. A strong peak was noted at 38.535° along with peaks at 44.563° and 77.860° due to aluminium being the primary matrix phase. The intermetallic phases AlNi and Al_3Ni were associated with the diffraction signals at 22.273°, 64.762°, and 40.112°, confirming that these compounds were formed in situ during the FS.

Such compounds have been described as especially beneficial, given that they improve the hardness, wear resistance, and chemical stability of aluminum-based coatings [42]. However, it must be noted that the overproduction of brittle phases, such as Al_3Ni, will decrease the toughness and increase the probability of cracking under service conditions [43, 44]. Thus, an optimal balance between aluminum as the matrix and intermetallic phases as reinforcements is critical to maximizing coating performance.

3.5. NC-IR Thermal Analysis

The necessary amount of heat from friction created due to the movement of the rod against the substrate contact is one of the necessities for correct depositing in FS. Figure 6 presents the temperature profile of Al7075-15Ni coating during FS using an NC-IR thermometer. According to the Figure, the temperature rose gradually throughout the early phase. Dwelling time and the beginning of the deposition produced rapid temperature increases, indicative of the presence of severe frictional heating at this time- indeed, the molecular diffusion created sufficient frictional heat. During the first 50 seconds, there was an abrupt temperature rise, peaking at nearly 370 °C during rapid plasticization of the consumable rod, followed by a gradual decline in temperature due to dissipated heat from the surroundings during process stabilization. The thermal response indicates the heating and cooling cycles that govern intermetallic formation, material flow, and finally the quality of the deposited layer. Another significant effect of this thermal profile is uniform plastic flow, which is important for obtaining flawless coatings [45, 46]. This peak temperature softens the consumable just enough within 40-60 seconds for redistribution and coating thickness to be equally developed. The temperature sharply increases and peaks within the first 5-60 seconds after deposition, which is the most active state of plasticization. Thereafter, temperatures commonly remain stable or show a slight decrease because the thermal equilibrium is established and substrate absorption occurs. By the end stage of the coating process, the interface temperature reaches about 290°C -300 °C, denoting the transition into the cooling phase of the deposited layer.

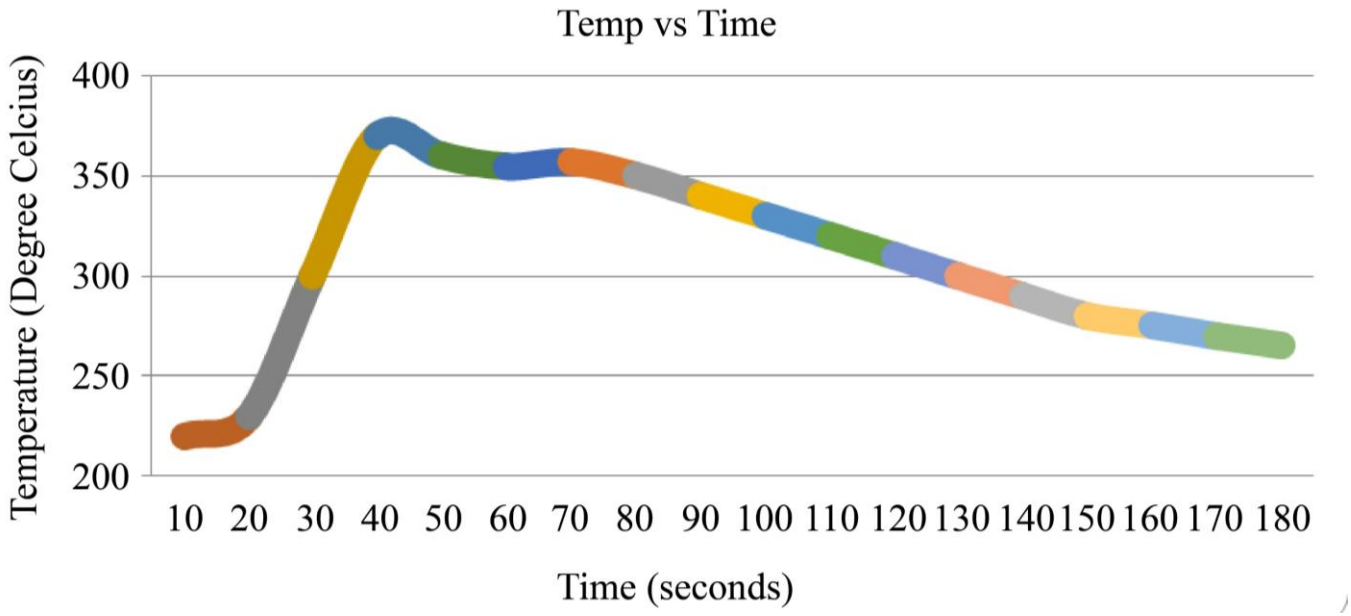

Fig. 6 Interface temperature vs time during the FS process

4. Conclusions with Limitations and Future Scope

- Thermomechanical effects occurring at the interface lead to the formation of a layer characterized by properties derived from the substrate and from the deposited coating. The coating-substrate bond system, due to intermetallic bonding from diffusion, will further help in the formation of a MMC composite structure at the interface.
- In the optimization study, it was found that only certain parameter combinations yielded acceptable deposits in FS. Under the pressure of 5 bar, rotation speeds of 1300 rpm -1500 rpm, and feed rates of 50-60 mm/min, the best results with continuous and uniform coatings were obtained. Any parameter setting above or below these

ranges yielded discontinuous, thin, and/or irregular deposits. Thus, it is evident that the deposition process must be under balanced process conditions.

- The dimensional characteristics and overall quality of the coating are strongly governed by the interaction of process parameters. A clear correlation exists between coating thickness and the applied forging force, where a reduction in force promotes greater coating thickness, while higher forces produce thinner deposits. Moreover, if the spindle speed is increased with a high feed rate, too little frictional heat is generated, which is detrimental to deposition, and discontinuities and delamination are frequently observable in the coating layer.
- The temperature readouts of the FS process show an abrupt increase in temperature during dwell time. In the deposition stage, the contact temperature, which lies in the range of 300 °C to 360 °C, is crucial to sustaining homogeneous plastic flow of the consumable material across the substrate.

4.1. Limitations

This study explores the FS of Al7075-15Ni on mild steel within a limited range of process parameters using a Taguchi L9 Design. Although it is effective in indicating trends for the optimizing parameters, the chosen parameter window may not completely account for the complex interactions of parameters outside the chosen levels. Evaluation was primarily concerned with coating geometry, microstructural features, intermetallic formation, and thermal behavior, but did not consider mechanical performance metrics such as wear resistance, adhesion strength, and fatigue behavior.

Interface temperatures were measured through a non-contact infrared thermometer that measures the surface temperature rather than the subsurface thermal gradient. Single coating composition and substrate under consideration might limit direct applicability to other alloy systems.

4.2. Future Scope

For future and further research work, optimization could be explored on larger parameters with more advanced statistical or predictive models. Thorough mechanical, tribological, and corrosion studies are needed to understand structure-property relationships. This could further include numerical thermal modelling and advanced microstructural characterization techniques for improved insight into diffusion mechanisms and phase evolutions. All these are highly relevant from the industrial point of view for extending the study to more Al-Ni compositions, multilayer coatings, and post-deposition treatments.

References

[1] Dillip Kumar Sahoo, P. Guna, and S. Deepan, "Performance Analysis on Deposition of Aluminium 6063 Over en8 Medium Carbon Steel by Friction Surfacing," *Materials Today: Proceedings*, vol. 64, pp. 116-123, 2022. [CrossRef] [Google Scholar] [Publisher Link]

[2] Gulmira Sh. Yar-Mukhamedova et al., "Advancements in Coating Methods and Properties of Titanium-Based Composite Coatings: A Review," *ES Materials and Manufacturing*, vol. 28, pp. 1-16, 2025. [CrossRef] [Google Scholar] [Publisher Link]

[3] Enhao Zhang et al., "Research Progress on Process Optimization of Thermal-Sprayed Iron-Based Amorphous Coatings," *Integrating Materials and Manufacturing Innovation*, vol. 14, pp. 247-275, 2025. [CrossRef] [Google Scholar] [Publisher Link]

[4] Ebrahim Seidi, and Scott F. Miller, "A Novel Approach to Friction Surfacing: Experimental Analysis of Deposition from Radial Surface of a Consumable Tool," *Coatings*, vol. 10, no. 11, pp. 1-17, 2020. [CrossRef] [Google Scholar] [Publisher Link]

[5] Seyedeh Marjan Bararpour, Hamed Jamshidi Aval, and Roohollah Jamaati, "Combined Experimental-Numerical Analysis of A356 Aluminum Alloy Friction Surfacing on AA2024 Aluminum Alloy Substrate," *Journal of Materials Research and Technology*, vol. 25, pp. 4860-4875, 2023. [CrossRef] [Google Scholar] [Publisher Link]

[6] R. George Sahaya Nixon, B.S. Mohanty, and R. Sathish, "Friction Surfacing of AISI 316 Over Mild Steel: A Characteriation Study," *Defence Technology*, vol. 14, no. 4, pp. 306-312, 2018. [CrossRef] [Google Scholar] [Publisher Link]

[7] Rajat Gupta, and Lalit Thakur, "A Study of Parametric Optimization, Microstructure and Wear Behavior of an AA7075–SiC Composite Coating Developed by Friction Surfacing," *Journal of Adhesion Science and Technology*, vol. 38, no. 12, pp. 2166-2190, 2024, [CrossRef] [Google Scholar] [Publisher Link]

[8] V. Fitseva, S. Hanke, and J. F. Dos Santos, "Influence of Rotational Speed on Process Characteristics in Friction Surfacing of Ti-6Al-4V," *Materials and Manufacturing Processes*, vol. 32, no. 5, pp. 557-563, 2017. [CrossRef] [Google Scholar] [Publisher Link]

[9] N.V. Chithra, "Effect of Reinforcement Addition on Mechanical Behavior of Al MMC - A Critical Review," *Journal of Environmental Nanotechnology*, vol. 13, no. 2, pp. 65-79, 2024. [CrossRef] [Google Scholar] [Publisher Link]

[10] S. Ganeshkumar, and S. Venkatesh, "Manufacturing Techniques and Applications of Multifunctional Metal Matrix Composites," *Functional Composite Materials: Manufacturing Technology and Experimental Application*, pp. 157-167, 2022. [CrossRef] [Google Scholar] [Publisher Link]

[11] M. Ravikumar et al., "Experimental Studies and Optimisation of Machining Performance Measurement for Al7075/n-SiCp Composite by using RSM and ANN Techniques," *Canadian Metallurgical Quarterly*, pp. 1-14, 2025. [CrossRef] [Google Scholar] [Publisher Link]

[12] Pawel Jozwik, Wojciech Polkowski, and Zbigniew Bojar, "Applications of Ni3al Based Intermetallic Alloys—Current Stage and Potential Perceptivities," *Materials*, vol. 8, no. 5, pp. 2537-2568, 2015. [CrossRef] [Google Scholar] [Publisher Link]

[13] Liming Ke et al., "Al–Ni Intermetallic Composites Produced in Situ by Friction Stir Processing," *Journal of Alloys and Compounds*, vol. 503, no. 2, pp. 494-499, 2010. [CrossRef] [Google Scholar] [Publisher Link]

[14] J. Gandra, R.M. Miranda, and P. Vilaça, "Performance Analysis of Friction Surfacing," *Journal of Materials Processing Technology*, vol. 212, no. 8, pp. 1676-1686, 2012. [CrossRef] [Google Scholar] [Publisher Link]

[15] Ravi Butola et al., "Fabrication and Multi-objective Optimization of Friction Stir Processed Aluminium based Surface Composites using Taguchi Approach," *Surface Topography: Metrology and Properties*, vol. 9, no. 2, 2021. [CrossRef] [Google Scholar] [Publisher Link]

[16] Guangliang Zhang et al., "Laser Cladding Al/Ni Composite Coating and its Tribology Performance," *Surface Engineering*, vol. 41, no. 2, pp. 266-278, 2025. [CrossRef] [Google Scholar] [Publisher Link]

[17] Bodala Raja Sekhar et al., "Wear Characteristic of TiC Coated AISI 1020 Mild Steel Fabricated by TIG Cladding Method," *Materials Today: Proceedings*, vol. 26, pp. 3288-3291, 2020. [CrossRef] [Google Scholar] [Publisher Link]

[18] Peng Yu et al., "Formation of Al3Ni Nanofibers in an Al-Based Metal Matrix Composite Fabricated by Reaction Sintering," *Journal of Materials Research*, vol. 19, no. 4, pp. 1187-1196, 2004. [CrossRef] [Google Scholar] [Publisher Link]

[19] U. Ashok Kumar, Bharadwaj Kasi, and P. Laxminarayana, "Optimization of Friction Surfacing Process Parameters on Low Carbon Steel Using Taguchi Approach," *Materials Science Forum*, vol. 969, pp. 691-696, 2019. [CrossRef] [Google Scholar] [Publisher Link]

[20] Rajat Gupta, and Lalit Thakur, "Development of an AA 7075 Wear-Resistant Coating on AA 6082 via Friction Surfacing: Optimization and Characterization," *Journal of Materials Engineering and Performance*, vol. 32, pp. 10311-10325, 2023. [CrossRef] [Google Scholar] [Publisher Link]

[21] Seyedeh Marjan Bararpour, Hamed Jamshidi Aval, and Roohollah Jamaati, "Modeling and Experimental Investigation on Friction Surfacing of Aluminum Alloys," *Journal of Alloys and Compounds*, vol. 805, pp. 57-68, 2019. [CrossRef] [Google Scholar] [Publisher Link]

[22] Ebrahim Seidi, and Scott F. Miller, "Lateral Friction Surfacing: Experimental and Metallurgical Analysis of Different Aluminum Alloy Depositions," *Journal of Materials Research and Technology*, vol. 15, pp. 5948-5967, 2021. [CrossRef] [Google Scholar] [Publisher Link]

[23] Parisa Pirhayati, and Hamed Jamshidi Aval, "An Investigation on Thermo-Mechanical and Microstructural Issues in Friction Surfacing of Al–Cu Aluminum Alloys," *Materials Research Express*, vol. 6, no. 5, 2019. [CrossRef] [Google Scholar] [Publisher Link]

[24] Márcio Levi Kramer de Macedo et al., "Deposit by Friction Surfacing and its Applications," *Welding International*, vol. 24, no. 6, pp. 422-431, 2010. [CrossRef] [Google Scholar] [Publisher Link]

[25] J. J. S. Dilip et al., "Use of Friction Surfacing for Additive Manufacturing," *Materials and Manufacturing Processes*, vol. 28, no. 2, pp. 189-194, 2013. [CrossRef] [Google Scholar] [Publisher Link]

[26] A.W. Batchelor et al., "The Effect of Metal Type and Multi-Layering on Friction Surfacing," *Journal of Materials Processing Technology*, vol. 57, no. 1-2, pp. 172-181, 1996. [CrossRef] [Google Scholar] [Publisher Link]

[27] Y. Aiman, S. Syahrullail, and M.K.A. Hamid, "Optimisation of Friction Surfacing Process Parameters for a1100 Aluminium Utilising Different Derivatives of Palm Oil based on Closed Forging Test," *Biomass Conversion and Biorefinery*, vol. 14, pp. 8857-8874, 2024. [CrossRef] [Google Scholar] [Publisher Link]

[28] Arne Roos et al., "Friction Surfacing of Aluminum to Steel: Influence of Different Substrate Surface Topographies," *Materials & Design*, vol. 235, pp. 1-12, 2023. [CrossRef] [Google Scholar] [Publisher Link]

[29] K. Sri Ram Vikas et al., "Influence of Heat Treatments on Microstructural and Mechanical Properties of Grade 5 Titanium Friction Welds," *Engineering Research Express*, vol. 4, no. 2, 2022. [CrossRef] [Google Scholar] [Publisher Link]

[30] J.C. Galvis et al., "Influence of Friction Surfacing Process Parameters to Deposit AA6351-T6 over AA5052-H32 using Conventional Milling Machine," *Journal of Materials Processing Technology*, vol. 245, pp. 91-105, 2017. [CrossRef] [Google Scholar] [Publisher Link]

[31] X.P. Tao et al., "Effect of Fe and Ni Contents on Microstructure and Wear Resistance of Aluminum Bronze Coatings on 316 Stainless Steel by Laser Cladding," *Surface and Coatings Technology*, vol. 342, pp. 76-84, 2018. [CrossRef] [Google Scholar] [Publisher Link]

[32] Lijia Zhao et al., "Effect of Particle Size on Ceramic Particle Content in Cold Sprayed Al-Based Metal Matrix Composite Coating," *Journal of Thermal Spray Technology*, vol. 31, pp. 2505-2516, 2022. [CrossRef] [Google Scholar] [Publisher Link]

[33] Ramezanali Farajollahi, Hamed Jamshidi Aval, and Roohollah Jamaati, "Effect of Friction Surfacing Parameters on the Microstructural, Mechanical Properties, and Wear Characteristic of Al-Cu-Mg Alloy Coating Reinforced by Nickel Aluminide," *Archives of Civil and Mechanical Engineering*, vol. 22, 2022. [CrossRef] [Google Scholar] [Publisher Link]

[34] P. Azhagarsamy, K. Sekar, and K. P. Murali, "Nickel Aluminide Intermetallic Composites Fabricated by Various Processing Routes – A Review," *Materials Science and Technology*, vol. 38, no. 9, pp. 556-571, 2022. [CrossRef] [Google Scholar] [Publisher Link]

[35] D. Prince Sahaya Sudherson et al., "Experimental Investigation on Corrosion Behavior of Friction Surfaced Mild Steel with Aluminum Alloy 5083-Cadmium Composite," *Materials Research Express*, vol. 6, no. 8, 2019. [CrossRef] [Google Scholar] [Publisher Link]

[36] Armi Tabaghi, Hossein Tavakoli, and Abdolvahed Kami, "Deposition of an Al/SiC Composite Coating on Steel by Friction Surfacing: Corrosion and Wear Properties," *Mechanics of Advanced Composite Structures*, vol. 9, no. 2, pp. 287-296, 2022. [CrossRef] [Google Scholar] [Publisher Link]

[37] K.H.S. Silva et al., "The Behaviour of AISI 4340 Steel Coatings on Low Carbon Steel Substrate Produced by Friction Surfacing," *Surface and Coatings Technology*, vol. 399, 2020. [CrossRef] [Google Scholar] [Publisher Link]

[38] Zina Kallien et al., "Application of Friction Surfacing for Solid State Additive Manufacturing of Cylindrical Shell Structures," *Additive Manufacturing Letters*, vol. 8, pp. 1-8, 2024. [CrossRef] [Google Scholar] [Publisher Link]

[39] Rajat Gupta, and Lalit Thakur, "Influence of Micro-Sized Al_2O_3 Particles on Mechanical and Wear Performance of an AA7075-Al2O3 Composite Coating Developed by Friction Surfacing," *International Journal on Interactive Design and Manufacturing*, vol. 18, pp. 5583-5597, 2024. [CrossRef] [Google Scholar] [Publisher Link]

[40] Nartu Mohan Sai Kiran Kumar Yadav et al., "Friction Surface Layer Deposition of Triple-phase $Al_{10}Cr_{12}Fe_{35}Mn_{23}Ni_{20}$ High Entropy Alloy: Process Optimization and Microstructural Evolution," *Materials Science and Engineering: A*, vol. 927, pp. 1-37, 2025. [CrossRef] [Google Scholar] [Publisher Link]

[41] Noah E. El-Zathry et al., "Friction Stir-Based Techniques: An Overview," *Welding in the World*, vol. 69, pp. 327-361, 2025. [CrossRef] [Google Scholar] [Publisher Link]

[42] B. M. Karthik et al., "Effect of Weight of Reinforcement and Coating Thickness on the Hardness of Stir Cast AL7075–Nickel Coated Duralumin Powder MMC," *Journal of Applied Engineering Science*, vol. 20, no. 3, pp. 900-907, 2022. [CrossRef] [Google Scholar] [Publisher Link]

[43] Xun He, Xiao Peng, and Juan Fang, "Study on the Microstructure and High-Temperature Oxidation Performance of β-NiAl/γ′-Ni_3Al Intermetallic Compounds Fabricated by Laser Metal Deposition," *Metals*, vol. 13, no. 8, pp. 1-11, 2023. [CrossRef] [Google Scholar] [Publisher Link]

[44] D. Guo et al., "Friction Surfacing of AISI 904L Super Austenitic Stainless Steel Coatings: Microstructure and Properties," *Surface and Coatings Technology*, vol. 408, 2021. [CrossRef] [Google Scholar] [Publisher Link]

[45] Aishwarya Deshpande et al., "Fully Consolidated Deposits From Oxide Dispersion Strengthened and Silicon Steel Powders Via Friction Surfacing," *Journal of Manufacturing Science and Engineering*, vol. 146, no. 10, pp. 1-9, 2024. [CrossRef] [Google Scholar] [Publisher Link]

[46] Marius Hoffmann, Arne Roos, and Benjamin Klusemann, "Friction Surfacing of Aluminum Alloys on Ti6Al4V - Investigation of Process Parameters, Material Deposition Behavior and Bonding Mechanisms," *Surface and Coatings Technology*, vol. 503, pp. 1-12, 2025. [CrossRef] [Google Scholar] [Publisher Link]